Dissociation between Temporal and Spatial Anticipation in the Neural Dynamics of Goal-directed Movement Preparation

Cesar Augusto Canaveral, Félix-Antoine Savoie, Frédéric Danion, Pierre-Michel Bernier

Dissociation between Temporal and Spatial Anticipation in the Neural Dynamics of Goal-directed Movement Preparation

Cesar Augusto Canaveral[1], Félix-Antoine Savoie[1], Frédéric R. Danion[2], and Pierre-Michel Bernier[1]

Abstract

■ It is well documented that providing advanced information regarding the spatial location of a target stimulus (i.e., spatial anticipation) or its timing of occurrence (i.e., temporal anticipation) influences reach preparation, reducing RTs. Yet, it remains unknown whether the RT gains attributable to temporal and spatial anticipation are subtended by similar preparatory dynamics. Here, this issue is addressed in humans by investigating EEG beta-band activity during reach preparation. Participants performed a reach RT task in which they initiated a movement as fast as possible toward visual targets following their appearance. Temporal anticipation was manipulated by having the target appear after a constant or variable delay period, whereas spatial anticipation was manipulated by precueing participants about the upcoming target location in advance or not. Results revealed that temporal and spatial anticipation both reduced reach RTs, with no interaction. Interestingly, temporal and spatial anticipation were associated with fundamentally different patterns of beta-band modulations. Temporal anticipation was associated with beta-band desynchronization over contralateral sensorimotor regions specifically around the expected moment of target onset, the magnitude of which was correlated with RT modulations across participants. In contrast, spatial anticipation did not influence sensorimotor activity but rather led to increased beta-band power over bilateral parieto-occipital regions during the entire delay period. These results argue for distinct states of preparation incurred by temporal and spatial anticipation. In particular, sensorimotor beta-band desynchronization may reflect the timely disinhibition of movement-related neuronal ensembles at the expected time of movement initiation, without reflecting its spatial parameters per se. ■

INTRODUCTION

The time necessary to initiate a reaching movement toward an appearing stimulus, referred to as RT, is known to be influenced by prior knowledge as to when and where it will appear. In support, studies manipulating the temporal predictability of an impending target have shown that RTs are faster when the timing of movement initiation is predictable as compared with when it is not (i.e., temporal anticipation; Johari & Behroozmand, 2017; Nobre, Correa, & Coull, 2007; Niemi & Näätänen, 1981; Alegria, 1975). Similarly, studies manipulating the number of possible reach target locations have shown that RTs are faster when the direction of the movement is specified in advance as compared with when it is not (i.e., spatial anticipation; Schmidt & Lee, 2011; Hick, 1952). However, these two types of anticipation have largely been studied in isolation; thus, it remains unclear whether the gains in reach RT associated with spatial and temporal anticipation are subtended by similar preparatory dynamics at the neural level.

Interestingly, recent behavioral work suggests that the mechanisms involved in the directional specification of a reaching movement are independent from those mediating its initiation (Haith, Pakpoor, & Krakauer, 2016). Specifically, these authors compared RTs in a "standard" task in which participants initiated reaching movements after target presentation to a task in which they were forced to initiate movements with lower-than-normal RTs using rhythmic cues. They showed that, in the latter condition, RTs could be reduced by up to 80 msec, but critically, the directional accuracy of these movements was as good as in the standard task. These data suggest that the neural processes that mediate the initiation of the movement are not necessarily related to those that serve to specify the spatial component of the reach. In further support, electrophysiological work in monkeys showed that reach initiation is accompanied by a large change in neural activity in primary motor (M1) and dorsal premotor cortex, which reflects when the movement will occur, but which carries little information about reach direction (Kaufman et al., 2016). This indicates that separate "components" of the population response in these regions encode the direction of the reaching movement and the timing of movement initiation. In light of these results, it is possible that temporal and spatial anticipation, although both leading to gains in reach RT, may be associated with distinct neural preparatory dynamics.

Movement preparatory activity can be characterized with high temporal resolution using EEG, with known modulations

[1]Université de Sherbrooke, [2]Aix Marseille Université, CNRS, Institut de Neurosciences de la Timone

in many frequency bands. Most notable is the event-related desynchronization (ERD) in the beta-band (13–30 Hz) that is observed over contralateral sensorimotor regions before and during movement execution (Kilavik, Zaepffel, Brovelli, MacKay, & Riehle, 2013; Pfurtscheller & Lopes da Silva, 1999). Although beta-band ERD has long been linked to "motor readiness," there remains ambiguity as to whether it relates more to the timing of initiation of a reaching movement or to the specification of its spatial (i.e., directional) component. For one, the "status quo" hypothesis, according to which reduced power reflects a release from inhibition necessary for a change in motor state (Jenkinson & Brown, 2011; Perfetti et al., 2011; Engel & Fries, 2010; Gilbertson et al., 2005), suggests that beta-band ERD is closely tied to movement initiation (Khanna & Carmena, 2017). As such, movements for which the go-cue is rhythmic and thus predictable are associated with greater premovement beta-band ERD than when the go-cue is unpredictable (Alegre et al., 2003). This possibility is further supported by evidence relating beta-band oscillations to predictive timing (Arnal, 2012; Fujioka, Trainor, Large, & Ross, 2012; Saleh, Reimer, Penn, Ojakangas, & Hatsopoulos, 2010). However, there is also evidence that beta-band ERD is modulated by the degree of directional uncertainty of an upcoming reach, suggesting a possible role in encoding the spatial aspects of movements. For example, premovement beta-band ERD is greater when reducing the number of possible target directions (Tzagarakis, Ince, Leuthold, & Pellizzer, 2010) or the angle of separation between two alternative targets (Grent-'t-Jong, Oostenveld, Jensen, Medendorp, & Praamstra, 2014). Overall, these studies demonstrate that temporal and spatial precueing both influence the pattern of the beta-band ERD. However, direct comparison between temporal and spatial anticipation, as well as their possible interaction during reach preparation, has never been explicitly tested.

Here, this is addressed using a factorial design in a reach RT task. Temporal anticipation was manipulated by having separate blocks in which the delay period was either constant, thus predictable (i.e., 2 sec), or variable, thus less predictable (i.e., 1.25, 2, or 2.75 sec). Spatial anticipation was manipulated by using spatial precues that were either informative (i.e., one location) or noninformative (i.e., three possible locations) as to the upcoming target location. It was hypothesized that beta-band ERD would be largest when both the target timing and location are predictable (with RTs being lowest), moderate when only one of the two is predictable, and smallest when none are predictable (with RTs being highest).

METHODS

Participants

Twenty-seven young adults (23.1 ± 2.1 years old, 14 women and 13 men) without any known neurological or psychiatric condition took part in the experiment. They were all self-declared right-handed and had no visual impairment left uncorrected. All participants provided informed consent before the experiment by signing a consent form approved by the ethics committee of the Centre Hospitalier de l'Université de Sherbrooke, and they all received a monetary compensation of $20 (CAD) for their participation.

Apparatus

Participants sat comfortably facing a CRT monitor and a digitizing tablet (Figure 1A). The monitor (LG Studioworks 995E) was positioned ~77 cm in front of participants. The tablet (GTCO CalComp DB6 1218) was placed directly in front of them, and its position was held constant. The tablet recorded the position of a hand-held stylus in real time, which was presented as a cursor on the monitor (green circle; 0.5 cm in diameter; Figure 1B). Participants were instructed to control the cursor by sliding the stylus across the tablet with the right hand. A custom-made box covered the digitizing tablet, such that participants could not see their arm while moving.

Stimuli and Task

The experimental task consisted of center-out reaching movements toward one of three possible visual targets (see Figure 2). All movements were initiated from a starting circle (gray; 0.75 cm in diameter) located at the bottom of the screen. The targets (white circles; 1.65 cm in diameter) were situated 7 cm away from the starting circle, at 30°, 90°, and 150° relative to the trigonometric circle (i.e., rightward, straight ahead, and leftward relative to midline, respectively). Participants were required to gaze at a fixation cross (red; 0.3 × 0.3 cm) situated 4 cm above the starting circle throughout the entire experiment to prevent eye movements.

Figure 2 illustrates the sequence of events for a given trial. Participants brought the cursor into the starting circle to begin the trial. After a 0.5-sec baseline period, a precue specifying the possible locations of the targets was presented, marking the beginning of a delay period. At the end of the delay period, a target turned green (i.e., go-cue), prompting participants to perform their reach toward it. Participants were instructed to initiate and execute their movements as fast and accurately as possible. They were told not to stop on the target but to "strike" through it with a single uncorrected movement. After movement completion, participants were instructed to hold their final hand position for 250 msec, after which the cursor disappeared, prompting the return to the starting circle for the initiation of the next trial.

Experimental Design

The temporal and spatial anticipation of target onset were independently manipulated using a 2 × 2 factorial design (see Figure 2). Temporal anticipation was manipulated by

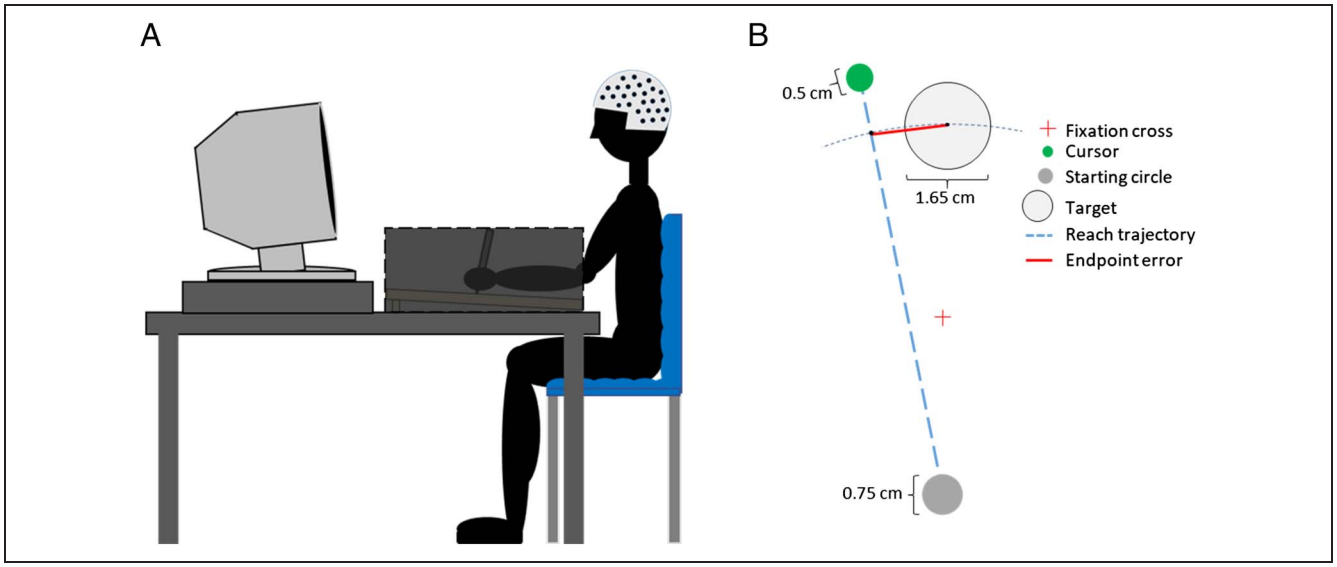

Figure 1. Schematic representation of experimental procedures. (A) Side view of the experimental setup. (B) Schematic view of cursor trajectory (blue trace) in a given trial. Endpoint error was calculated as the Euclidian distance (red trace) between the center of the cursor at the 7 cm radial distance and the center of the aiming target. Figure not to scale.

having participants take part in two separate experimental blocks in which the duration of the delay period was either constant at 2 sec (i.e., *One Timing*), or could vary pseudorandomly (i.e., no more than four subsequent trials with the same delay period) between three possibilities (i.e., 1.25, 2, or 2.75 sec; *Three Timings*). These temporal variations were determined after pilot testing. The objective of using repeated exposure to either constant or variable delay periods was to manipulate participants' expectancy of the go-cue to build an internal representation of the moment of target onset (Nobre et al., 2007). This way, it is assumed that a constant delay period would render the go-cue occurrence more predictable than a variable delay period and would reduce RTs (Johari & Behroozmand, 2017; Niemi & Näätänen, 1981; Alegria, 1975). Although different approaches could have been used to influence temporal anticipation, such as rhythmic entrainment to a tone (Alegre et al., 2003), here the rationale for building a temporal prior of target onset was to keep the preparatory period exempt of additional sensory stimuli (i.e., rhythmic tones), which would have themselves influenced oscillatory activity and made it difficult to compare EEG modulations across conditions. Thus, in the present context, preparatory activity was identical from a sensory standpoint across the two levels of temporal anticipation, therefore allowing to ascribe all spectral modulations to

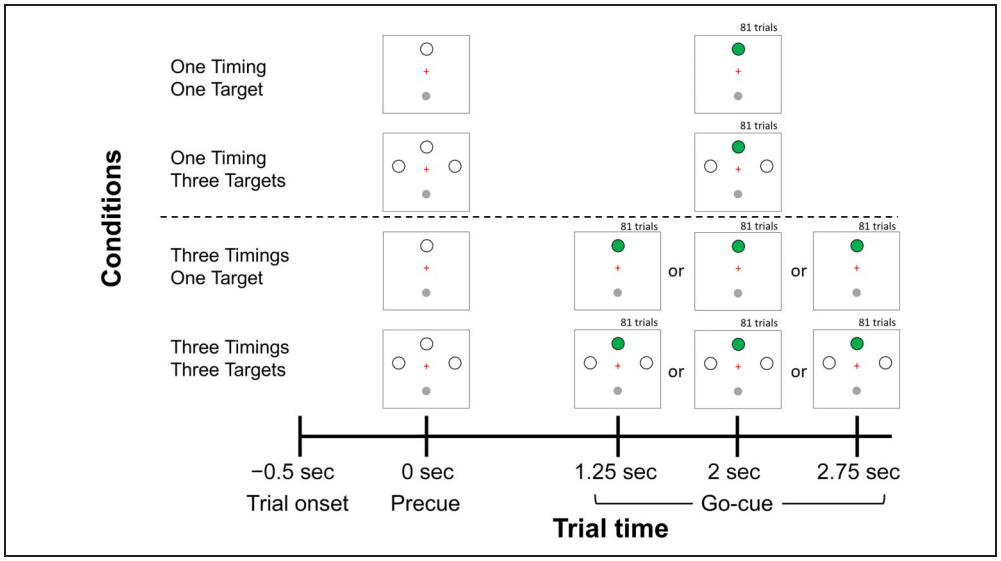

Figure 2. Trial sequence and experimental design. Temporal and spatial anticipation were manipulated in four experimental conditions: (1) *One Timing–One Target*; (2) *One Timing–Three Targets*; (3) *Three Timings–One Target*; (4) *Three Timings–Three Targets*. Trials started with a 0.5-sec baseline period, after which a precue was provided. The precue consisted in the presentation of either a single target or three targets. The two levels of the factor temporal anticipation were conducted in separate experimental blocks (*One Timing, Three Timings*). In the *One Timing* block (above the dotted line), the timing of the go-cue (*i.e.,* target turning green) was constant at 2 sec, whereas in the *Three Timings* block (below the dotted line), it varied between 1.25, 2, or 2.75 sec. Only trials for which the go-cue occurred at 2 sec were kept for primary experimental analysis (n = 81 per participant per condition).

movement preparation only. Importantly, the ordering of the two blocks was counterbalanced across participants to rule out any ordering effect in the behavioral and EEG results. There was no pause between experimental blocks.

Within each of the two experimental blocks, spatial anticipation was manipulated by having the precue being fully informative as to the spatial location of the upcoming target (i.e., *One Target*; straight ahead) or not (i.e., *Three Targets*; leftward, straight ahead, and rightward; see Figure 2). The experiment thus consisted of four distinct conditions.

In a first block, participants could be submitted to either the *One Timing–One Target* condition or the *One Timing–Three Targets* condition. This block comprised a total of 178 trials: 81 for the former and 81 for the later (i.e., 27 trials per target), as well as 16 no-go trials. No-go trials were identical to the other trials with the exception that the go-cue was not presented. Participants were informed of these trials and were instructed not to move in this context. These trials served to prevent participants from jumping the start and to ensure reactive behavior to the go-cue, which was especially relevant for the *One Timing–One Target* condition because both spatial and temporal information were known in advance. In a second block, participants could be submitted to either the *Three Timings–One Target* condition or the *Three Timings–Three Targets* condition. This block comprised a total of 510 trials: 243 for the former (i.e., 81 trials per possible timing) and 243 for the later (i.e., 81 trials per possible timing, comprising 27 trials per target), as well as 24 no-go trials. Trials were pseudorandomized throughout each experimental block. No-go trials also served to minimize the effect of the hazard function in the *Three Timings* conditions, which refers to the conditional probability that an event will occur given it has not yet occurred (Nobre et al., 2007; Luce, 1986). Overall, the experiment comprised 688 trials and lasted ~75 min. In addition, before the actual experiment, participants underwent a practice session of 40 random trials to familiarize with the experimental setup and task. These trials were not considered in any analyses.

By design, the *One Timing* conditions (*One Timing–One Target* and *One Timing–Three Targets*) consisted exclusively of trials with delay periods of 2 sec. Hence, the primary experimental strategy was to compare preparatory activity across all four conditions using only trials in which the delay period was 2 sec. Doing so ensured that the delay period was identical in every respect across the four conditions, such that any difference would be solely attributable to differential movement preparation incurred by temporal or spatial anticipation. In additional analyses, data from trials with delay periods of 2.75 sec were used to provide further validation of the results obtained in the main 2-sec delay period analysis.

To ensure that an internal representation of the timing of target onset (i.e., prior) would be achieved through repeated exposure to either constant or variable delay periods (temporal anticipation factor), it was decided a priori that the first 12 trials of each of the two *One Timing* conditions (*One Timing–One Target* and *One Timing–Three Targets*) would serve as "training" trials and be discarded, as well as the first 36 trials of each of the two *Three Timings* conditions (12 trials per possible timing in both the *Three Timings–One Target* and *Three Timings–Three Targets* conditions). This corresponded to 96 trials out of the 688 per participant (14% of the trials).

Behavioral Data Recording and Analysis

Visual stimuli were presented using functions from the psychophysics toolbox (Psychtoolbox; Brainard, 1997; Pelli, 1997), which were run with MATLAB (v2014a, The MathWorks) using the Windows 7 operating system (Microsoft) on a desktop computer (Dell Optiplex 7010). All hand position-related data, obtained from the digitizing tablet, were recorded at 100 Hz and analyzed off-line with custom MATLAB routines. Movement initiation was defined as the first time sample when the cursor fell completely outside the starting circle (i.e., the cursor and starting circle did not overlap). RT was calculated as the time difference between the go-cue and movement initiation. Reach duration was calculated as the time difference between movement initiation and the first time sample when the radial distance between the centroids of the cursor and the starting circle exceeded 7 cm (i.e., the target distance). Endpoint error was defined as the Euclidian distance in centimeters (thus in absolute terms) between the centroid of the cursor at the 7 cm radial distance and the aiming target (see red trace in Figure 1B).

Outlier trials were rejected based on several criteria. First, trials for which (1) RT was under 160 or over 600 msec, (2) reach duration exceeded 500 msec, or (3) endpoint error was greater than 5 cm were discarded. In addition, trials for which RT and reach duration were beyond ± 2 *SD* from a participant's mean were rejected. All these criteria led to the rejection of 21 ± 14 trials per participant (3.5% of the data).

EEG Data Acquisition, Processing, and Time–Frequency Decomposition

EEG Recording and Analysis

Scalp EEG data were recorded from a 64-electrode actiCAP (Brain Products) and BrainAmp system (Brain Products). Electrodes were positioned in accordance with the extended 10/20 system (Falk Minow Services), and it was ensured that the Cz electrode was at the participant's vertex. The reference electrode was located at FCz, and impedances were kept below 20 kΩ. The EEG signals were digitized online (sampling rate 500 Hz; BrainVision Recorder

2.0) using a Laptop (Dell Latitude E6530) running on Windows 7 (Microsoft).

All EEG analyses were done off-line using custom MATLAB routines, as well as functions derived from the EEGLAB toolbox (Delorme & Makeig, 2004). First, trials that had been rejected based on movement kinematics were discarded from the EEG data sets. Then, data were digitally bandpass-filtered between 1 and 55 Hz and epoched from −1000 to +3000 msec around precue onset for all conditions. EEG data were then baseline-corrected to the average potential recorded during the 500 msec preceding the precue. This period was chosen as a baseline because participants were motionless and the precue had not been presented yet. Cortical activity was thus considered neutral at that moment. Thereafter, EEG epochs showing voltage values exceeding ± 80 μV were discarded. Based on this criterion, 47 ± 55 trials per participant (6.8% of data) were discarded from further behavioral and EEG analyses.

In summary, after considering both kinematic-based and EEG-based trial rejections, all analyses (both EEG and movement kinematics) were conducted on a total of 62 ± 8, 64 ± 7, 60 ± 9, and 63 ± 8 trials per participant for *One Timing–One Target*, *One Timing–Three Targets*, *Three Timings–One Target*, and *Three Timings–Three Targets*, respectively.

The data were further inspected for artifacts with a procedure based on independent component (IC) analysis, a blind separation technique that decomposes the EEG signal into maximally ICs to remove artifacts from EEG activity without having to discard entire epochs (Gwin & Ferris, 2012a, 2012b; Gwin, Gramann, Makeig, & Ferris, 2010; Hammon, Makeig, Poizner, Todorov, & De Sa, 2008; Delorme & Makeig, 2004; Makeig et al., 2002). The *runica* function in EEGLAB was applied to decompose EEG signals into statistically maximal ICs. ICs were analyzed with respect to scalp topography and frequency characteristics and were identified as being artifactual and removed if their scalp map showed activity concentrated at the far edges of the scalp, which are often indicative of muscle and/or ocular artifacts (Jung et al., 2000) or if they met one of the following two criteria: (1) their time course showed spurious bursts of activity and (2) their spectral power did not generally decrease as a function of frequency, as expected for EEG spectral power (Buzsáki, 2006). Cleaned EEG data were generated by projecting back the time course of activity of the remaining ICs to the electrode space.

To assess time–frequency power modulations across experimental conditions, the EEG time series of each electrode and trial were convolved with a series of complex Morlet wavelets (1–50 Hz, 1-Hz steps). Spectral power estimates were obtained by multiplying the resulting complex signal by its complex conjugate. Wavelet cycles were linearly increased from 3 to 7.9 in 0.1 steps to improve frequency resolution at higher frequencies (Cohen, 2014). The obtained power time series were then baseline-normalized, and changes in power were expressed in decibels as follows:

$$\mathrm{dB} = 10 \log_{10}\left(\frac{RP}{\bar{BP}}\right)$$

where dB corresponds to the decibel-converted mean power, RP corresponds to the mean power value at a given time point, and $\bar{BP}$ corresponds to the average raw power during the baseline period, which was defined as the average power during the 500 msec preceding the precue. This measure was computed separately for each condition. Finally, the spectral power data were downsampled to 125 Hz.

Behavioral Statistical Analysis

All behavioral dependent variables (i.e., RT, reach duration, and endpoint error) were submitted to separate 2 Temporal Anticipation (*One timing*, *Three timings*) × 2 Spatial Anticipation (*One target*, *Three targets*) repeated-measures ANOVAs. All statistical tests were two-tailed, and the threshold for significance was set to .05. Data normality was tested with the Shapiro–Wilk test before all analyses. The statistical analysis of the all behavioral dependent variables was done with IBM SPSS statistics (Version 23, IBM Canada). For all these analyses, the F statistic, statistical significance (p), effect size (η_p^2; Field, 2009), and descriptive statistics (mean ± *SEM*) are reported in the text. According to Fritz, Morris, and Richler (2012), the thresholds past which η_p^2 denotes small, moderate, and large effect sizes are .01, .06, and .14, respectively (Fritz et al., 2012).

EEG Statistical Analysis

Regarding EEG data, the goal was to assess whether beta-band (data averaged over 13–30 Hz) power during the delay period was modulated by either temporal or spatial anticipation. To do so, nonparametric permutation tests were conducted to identify clusters of spatially and temporally adjacent electrode/time pairs showing statistically significant differences across conditions (Maris & Oostenveld, 2007). This method does not make assumptions about the distribution of the data, and it provides an efficient solution to the multiple comparisons problem, making it particularly interesting for EEG analysis. Specifically, for each comparison, two-tailed dependent t tests were computed for all electrode/time pairs in the true EEG data. Adjacent electrode/time pairs whose test statistic exceeded statistical significance threshold, $t(26) = 2.056$, $\alpha = 0.05$, two-tailed, were then identified. To be considered as a cluster, at least three adjacent electrodes had to show statistically significant t values. The size of a cluster was obtained by summing the t values across all adjacent electrode/time pairs constituting the cluster. Then, permutations ($n = 1000$) were undertaken, which consisted

of randomly shuffling the experimental condition labels across participants. Following each permutation, the largest permuted cluster was identified. Ultimately, a Monte Carlo estimate (i.e., the proportion of permuted clusters whose size was larger than the clusters identified in the true data) was used to yield p values for each cluster.

All nonparametric permutation tests were conducted over the entire delay period starting from the precue (0 msec) until trial end (3000 msec). To probe for differences across the temporal anticipation factor, data were pooled across spatial anticipation levels, and dependent t tests were used to compare the *One Timing* to the *Three Timings* trials. Similarly, to probe for differences across the spatial anticipation factor, data were pooled across temporal anticipation levels, and dependent t tests were used to compare the *One Target* and *Three Targets* trials. To probe for an interaction between the two factors, dependent t tests were used to compare the differences between the *One Target* and *Three Targets* trials across the two temporal anticipation levels. Clusters were deemed statistically significant if their p value was smaller or equal to the significance threshold ($\alpha = .05$). All nonparametric permutation tests were done using the Fieldtrip toolbox (Oostenveld, Fries, Maris, & Schoffelen, 2011). For each identified cluster, the size, average statistic (t), statistical significance (p), and effect size (Cohen's d_z) are reported in the text. Cohen's d_z was calculated using the average t value of a cluster (Lakens, 2013; Rosenthal, 1984). According to Cohen (1988), d_z is considered small, moderate, or large if it exceeds 0.2, 0.5, or 0.8, respectively.

RESULTS

Behavioral Results

Mean RT data for all conditions can be seen in Figure 3A. The ANOVA conducted on the RT data revealed both a significant main effect of Temporal and Spatial Anticipation. Specifically, as can be seen in Figure 3B, RTs were significantly faster in *One Timing* (321 ± 5 msec) as compared with *Three Timings* (326 ± 5 msec), $F(1, 26) = 5.478$, $p = .027$, $\eta_p^2 = .174$. Similarly, as can be observed in Figure 3C, RTs were significantly faster in *One Target* (308 ± 5 msec) as compared with *Three Targets* (339 ± 5 msec), $F(1, 26) = 139.079$, $p < .001$, $\eta_p^2 = .842$. Importantly, there was no significant interaction between factors, $F(1, 26) = 0.279$, $p = .602$, $\eta_p^2 = .011$.

As an additional analysis, we assessed the effect of the different delay periods on RTs. Thus, a 3 (Delay Period; 1.25, 2, and 2.75 sec) × 2 (Spatial Anticipation; *One target*, *Three targets*) repeated-measures ANOVA was conducted on data from the *Three Timings* conditions only. This analysis revealed both a significant main effect of Delay Period, $F(1, 26) = 59.082$, $p < .001$, $\eta_p^2 = .694$, and Spatial Anticipation, $F(1, 26) = 118.540$, $p < .001$, $\eta_p^2 = .820$, but no interaction between factors, $F = 0.392$, $p = .537$, $\eta_p^2 = .014$. Specifically, when pooled across spatial anticipation levels, RTs in the 1.25-sec Delay Period (351 ± 4 msec) were significantly slower than in the 2-sec (326 ± 5 msec) and 2.75-sec (334 ± 5 msec) delay periods, with the latter being also significantly slower than in the 2-sec delay period (all t values ≥ 7.618 and all p values < .001). As for the spatial anticipation effect, results were consistent with the main

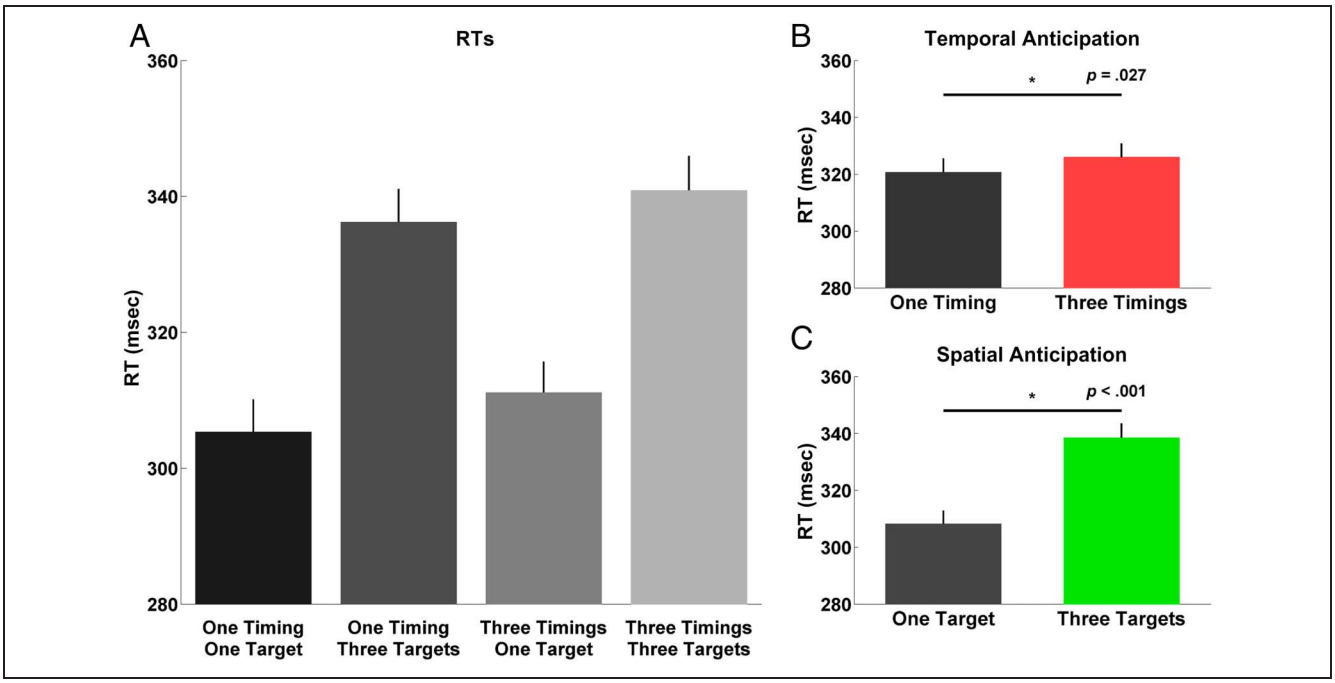

Figure 3. RTs. (A) Mean RTs in each of the four conditions using only trials for which the go-cue occurred at 2 sec. (B) Main effect of Temporal Anticipation. (C) Main effect of Spatial Anticipation. Error bars represent standard errors of the mean.

behavioral analysis, with RTs being significantly faster in *One Target* (324 ± 4 msec) as compared with *Three Targets* (350 ± 5 msec).

The ANOVA conducted on the reach duration data revealed both a significant main effect of Temporal and Spatial Anticipation. Specifically, reach duration was significantly lower for *One Timing* (85 ± 2 msec) than for *Three Timings* (88 ± 3 msec), $F(1, 26) = 5.651$, $p = .025$, $\eta_p^2 = .179$. Similarly, reach duration was significantly lower for *One Target* (85 ± 2 msec) than for *Three Targets* (88 ± 2 msec), $F(1, 26) = 9.048$, $p = .006$, $\eta_p^2 = .258$. There was no interaction between factors, $F(1, 26) = 1.452$, $p = .239$, $\eta_p^2 = .053$.

The ANOVA conducted on the endpoint error data revealed a significant main effect of Spatial Anticipation, with errors being significantly lower in *One Target* (0.508 ± 0.013 cm) as compared with *Three Targets* (0.592 ± 0.015 cm), $F(1, 26) = 9.048$, $p < .001$, $\eta_p^2 = .596$. There was neither a main effect of Temporal Anticipation, $F(1, 26) = 0.152$, $p = .700$, $\eta_p^2 = .006$, nor an interaction, $F(1, 26) = 0.106$, $p = .748$, $\eta_p^2 = .004$. An additional analysis comparing endpoint errors across the three targets (thus using only data from the *Three Targets* conditions) revealed that endpoint errors were greater for reaches toward the left (0.650 ± 0.014 cm) and right targets (0.610 ± 0.012 cm) as compared with reaches toward the central target (0.521 ± 0.007 cm; all t values ≥ 4.071 and all p values < .001). Endpoint errors did not differ significantly between the left and right targets, $t(1, 26) = 1.285$, $p = .210$.

Beta-band Power Results

The next analysis sought to investigate whether beta-band oscillatory power during the delay period was influenced by temporal and spatial anticipation or their interaction. For the temporal anticipation factor, as can be seen in Figure 4A, a large cluster was observed over left (contralateral) frontocentral, central, and centroparietal scalp sites (size = 1372.11, average $t = 3.04$, $p = .022$, $d_z = 0.59$). This cluster was significant only for a transient period of time between 968 and 1376 msec after the precue. To appreciate the directionality of this effect, Figure 4B presents the time course of beta-band activity across the two levels of the temporal anticipation factor, obtained by averaging data over the six electrodes presenting the largest number of significant time samples during the cluster period (FC1, FC3, C1, C3, CP1, and CP3; see inset for electrodes). As can be seen, beta-band power was significantly lower in *Three Timings* than in *One Timing* specifically around the moment of the first possible go-cue in the *Three Timings* conditions (i.e.,

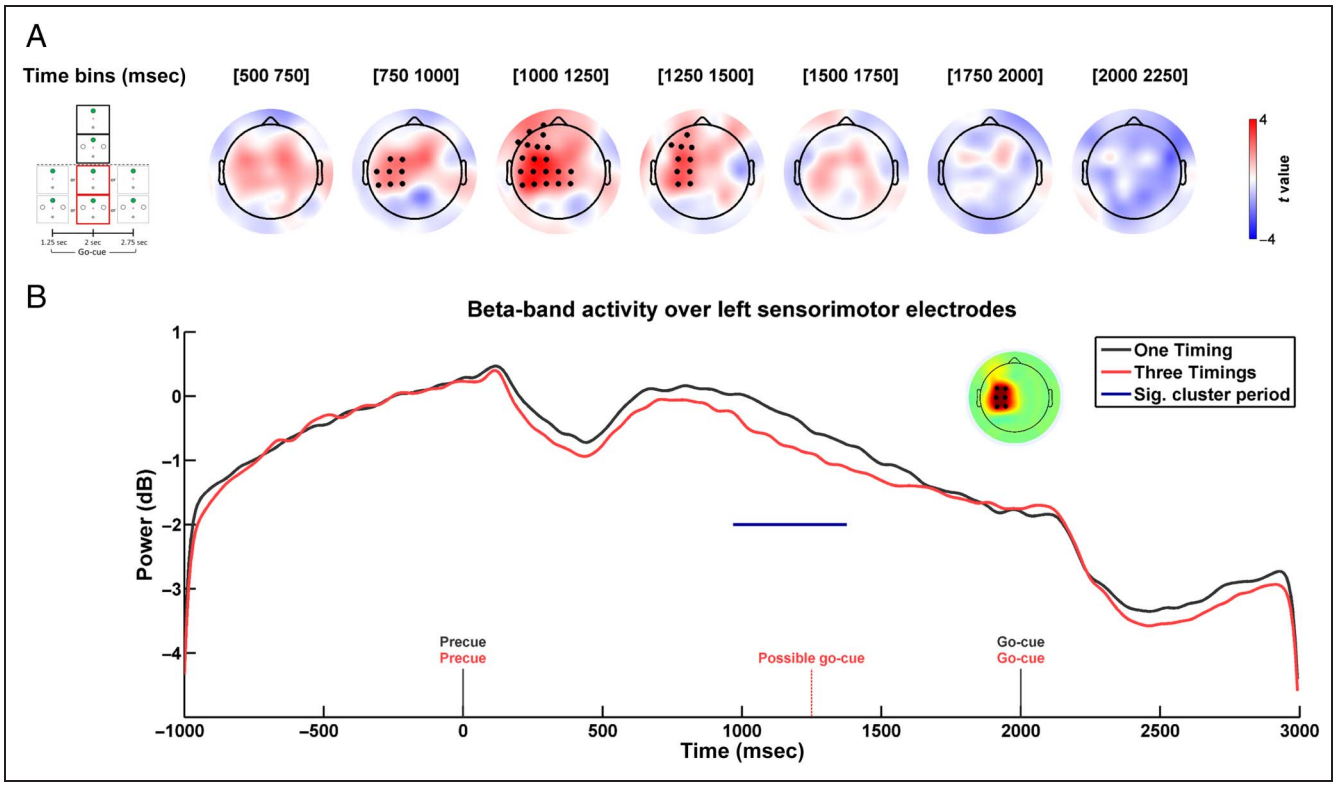

Figure 4. Main effect of Temporal Anticipation on beta-band power. (A) Paired comparisons of beta-band power across temporal anticipation levels during the delay period for trials in which the go-cue occurred at 2 sec (see inset). Black markers represent electrodes comprised in a significant cluster. (B) Beta-band power time course for *One Timing* conditions (black line) and *Three Timings* conditions (red line) during the delay period (obtained by averaging power values across the six electrodes presenting the largest number of significant time-samples during the cluster period; see inset). Horizontal blue line corresponds to the time period during which the cluster was significant ($p = .022$).

1250 msec). In other words, there was greater beta-band ERD over contralateral sensorimotor regions when there was a possibility that a go-cue would occur.

For the spatial anticipation factor, two significant clusters were identified (Figure 5A). They were observed bilaterally over occipital, parieto-occipital, parietal, and centro-parietal electrodes, although there was a right-hemisphere bias. The first cluster was observed between 136 and 568 msec after the precue (size = 5430.10, average $t = 4.45$, $p = .004$, $d_z = 0.86$), whereas the second cluster spanned between 640 and 2312 msec (size = 1250.53, average $t = 3.73$, $p = .002$, $d_z = 0.72$). To better visualize this effect, the temporal evolution of beta-band activity across the two levels of spatial anticipation are presented in Figure 5B. Time courses were produced by averaging beta-band power over the six electrodes presenting the largest number of significant time samples during the cluster periods (P1, Pz, P2, POz, PO4, and Oz; see inset for electrodes). As can be seen, beta-band power was significantly lower in *Three Targets* than in *One Target*. This effect was sustained over the major part of the delay period.

Finally, beta-band power differences between the two spatial anticipation levels (*One Target* vs. *Three Targets*) were compared across the temporal anticipation levels to probe for an interaction (see Experimental Design and Behavioral Statistical Analysis sections). This analysis revealed no significant interaction between factors (all clusters $p > .6$, one-tailed).

In summary, these results demonstrate that, even though temporal and spatial anticipation both incurred RT gains, they were subtended by different modulations in beta-band activity. Specifically, power in the left sensorimotor electrodes was only modulated by temporal anticipation, whereas power in parieto-occipital electrodes was only modulated by spatial anticipation.

Confirmatory Analysis

To provide further support for the above-mentioned pattern of results, additional analyses were performed using trials for which the go-cue was presented at 2.75 sec. Indeed, by using this new independent data set, it was possible to conduct similar contrasts as those conducted for the primary analysis.

First, to replicate the main effect of temporal anticipation, all trials in the *One Timing* conditions were contrasted to those in the *Three Timings* conditions for which the go-cue was presented at 2.75 sec (see inset of Figure 6A). This contrast engages the same neural

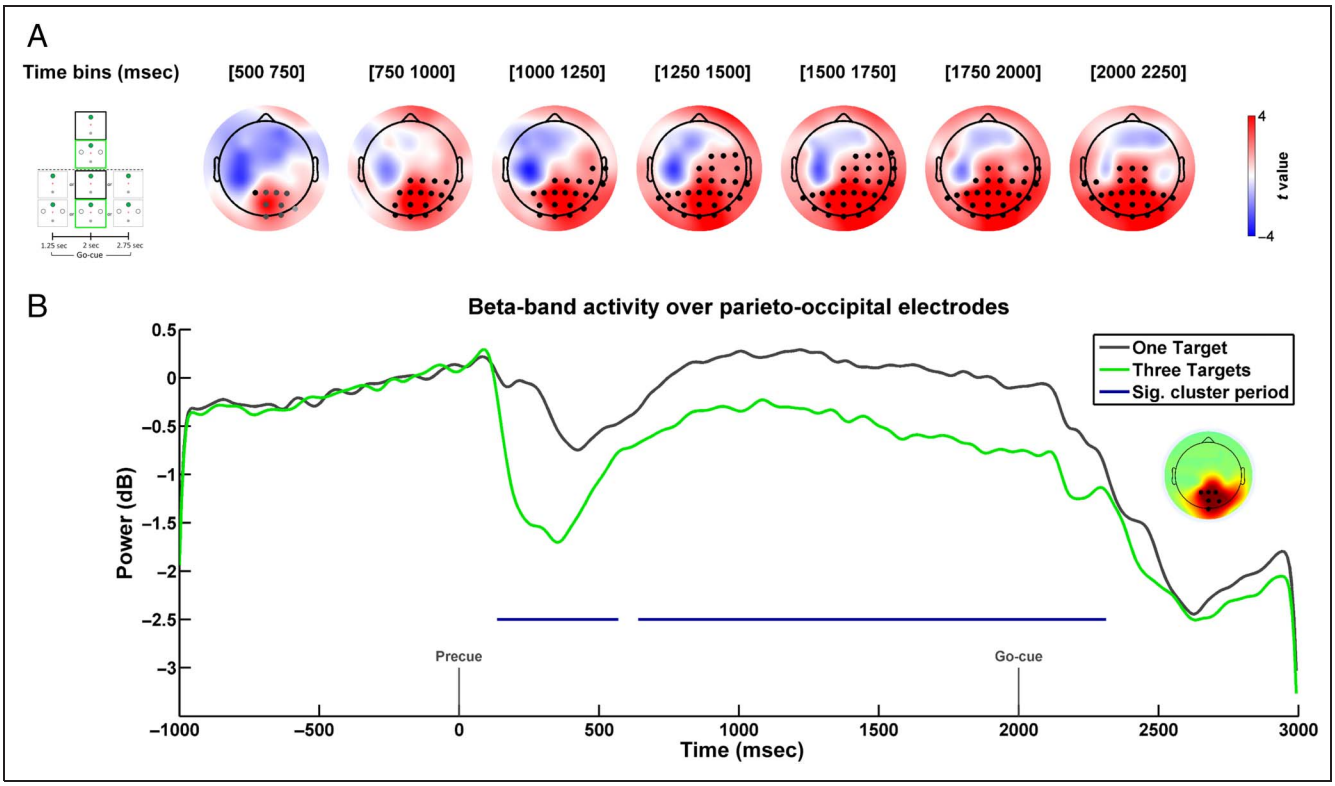

Figure 5. Main effect of Spatial Anticipation on beta-band power. (A) Paired comparisons of beta-band power across spatial anticipation levels during the delay period for trials in which the go-cue occurred at 2 sec (see inset). Black and pale gray markers represent distinct significant clusters, whereas dark gray markers denote electrodes common to both black and pale gray clusters (though at different time points). (B) Beta-band power time course for *One Target* conditions (black line) and *Three Targets* conditions (green line) during the delay period (obtained by averaging beta-band power values across the six electrodes presenting the largest number of significant time samples during the clusters periods; see inset). Horizontal blue lines correspond to time periods during which the clusters were significant (both $p < .004$).

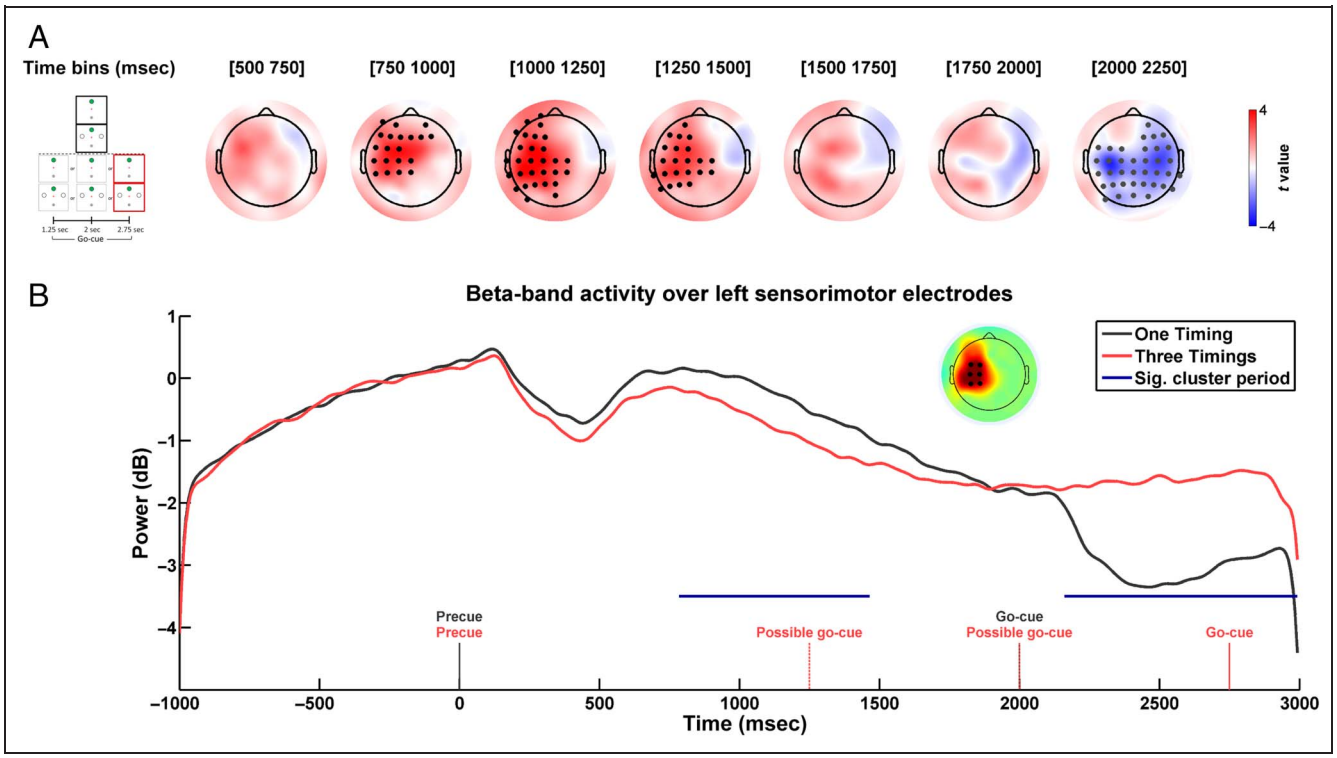

Figure 6. Additional analysis of the main effect of Temporal Anticipation on beta-band power. (A) Paired comparisons of beta-band power across temporal anticipation levels during the delay period for trials in which the go-cue occurred at 2 sec for *One Timing* conditions and at 2.75 sec for *Three Timings* conditions (see inset). Black markers represent significant positive clusters, whereas gray markers represent significant negative clusters. (B) Beta-band power time course for *One Timing* conditions (black line) and *Three Timings* conditions (red line) during the delay period (obtained by averaging beta-band power values across the six electrodes presenting the largest number of significant time samples during the clusters periods; see inset). Horizontal blue lines correspond to the time periods during which the clusters were significant ($p = .026$ and $p = .002$, respectively).

events as the original contrast until 2 sec, after which differences are expected because of the go-cue being presented only in the *One Timing* condition. Results were highly similar to those of the primary analysis. Specifically, as observed in Figure 6A, there was again a significant cluster over contralateral sensorimotor regions around the time of possible go-cue occurrence in the *Three Timings* conditions, from 784 to 1464 msec (size = 3601.45, average $t = 3.10$, $p = .026$, $d_z = 0.60$). As can be seen in the time courses of Figure 6B, the same six electrodes as in the primary analysis were found to contribute most to the cluster, revealing that beta-band power was significantly reduced in the *Three Timings* as compared with the *One Timing* conditions. As expected, after the presentation of the go-cue in the *One Timing* conditions at 2 sec, a second cluster was found over the same electrodes from 2160 to 2992 msec, showing much stronger beta-band ERD in *One Timing* than in *Three Timings* (size = −1884.56, average $t = -4.52$, $p = .002$, $d_z = 0.87$).

Second, to replicate the main effect of Spatial Anticipation, trials from the *Three Timings–One Target* condition for which the go-cue was presented at 2.75 sec were compared with trials from the *Three Timings–Three Targets* condition for which the go-cue was presented at 2.75 sec (see inset of Figure 7A). Again, this analysis revealed a very similar pattern of results as the primary analysis. As can be seen in Figure 7A, a large cluster over parieto-occipital electrodes was observed throughout the entire delay period until the go-cue, being significant between 120 and 2992 msec (size = 2.221.90, average $t = 3.99$, $p = .002$, $d_z = 0.76$). Once again, the same six electrodes as in the primary analysis were found to contribute most to the cluster, revealing that beta-band power was significantly lower in the *Three Targets* than in the *One Target* condition (Figure 7B).

Relationship between Beta-band Power and RT

The analyses conducted on beta-band power revealed a clear dissociation, with temporal anticipation being selectively associated with phasic modulations over left sensorimotor regions around moments of potential action and spatial anticipation being associated with tonic modulations over parieto-occipital regions over the entire delay period. An interesting contention is that these power modulations reflect distinct forms of preparation, which may be related to the RT gains incurred by each factor. To further probe the link between neural activity and RTs, we next assessed whether individual power differences between factor levels during the delay period could explain the RT modulations.

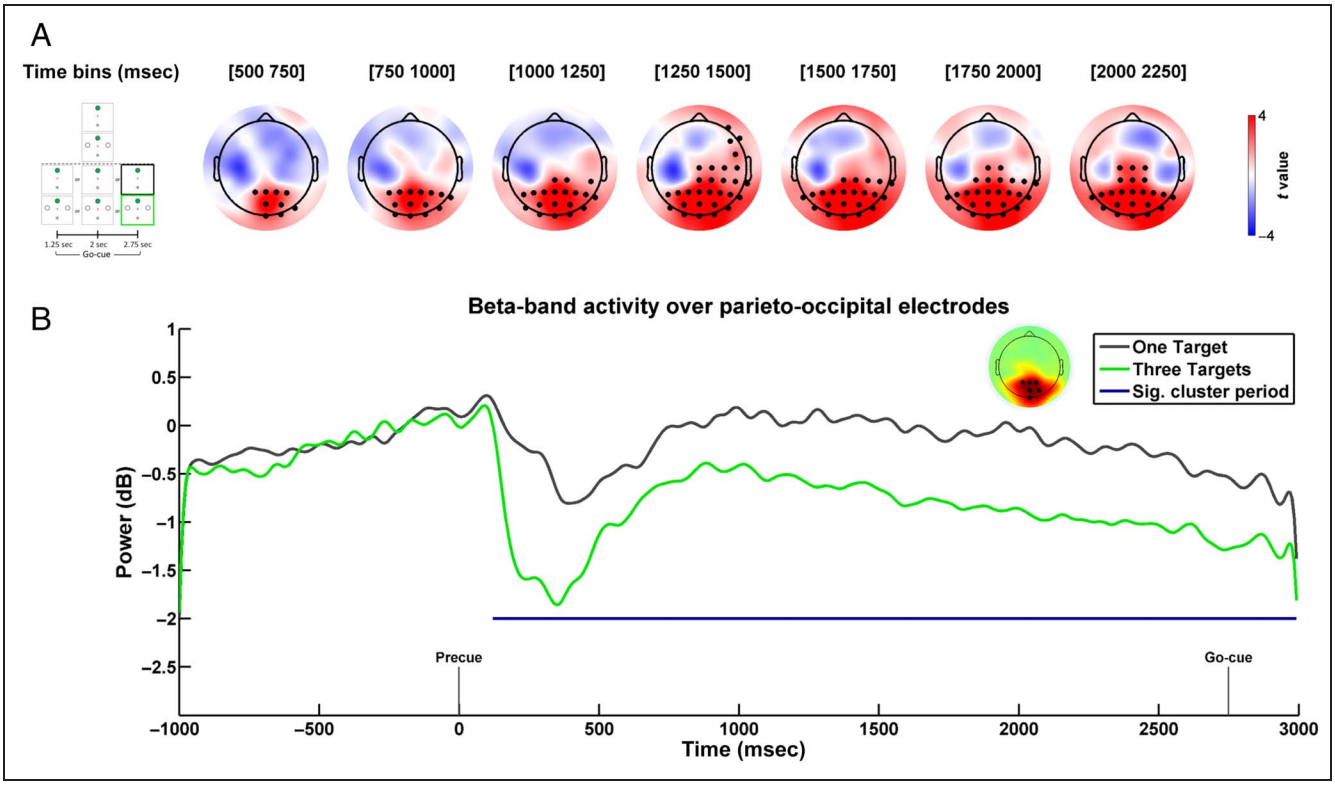

Figure 7. Additional analysis of the main effect of Spatial Anticipation on beta-band power. (A) Paired comparisons of beta-band power across spatial anticipation levels during the delay period for trials in which the go-cue occurred at 2.75 sec. (see inset). Black markers represent electrodes comprised in a significant cluster. (B) Beta-band power time course for *One Target* conditions (black line) and *Three Targets* conditions (green line) during the delay period (obtained by averaging beta-band power values across the six electrodes presenting the largest number of significant time samples during the clusters periods; see inset). Horizontal blue line corresponds to time period during which the clusters was significant ($p = .002$).

To do so, beta-band power differences were extracted from the six electrodes that most strongly contributed to the significant clusters identified between factor levels (see Figures 3B and 4B insets). The resulting differential time courses (*Three Timings* vs. *One Timing* and *Three Targets* vs. *One Target*) were then correlated at each time point with their corresponding RT differences. Thereafter, nonparametric analyses were used to identify significant correlation clusters, as described in the EEG Statistical Analysis section, with the two following variations. First, rather than dependent *t* tests, Spearman's rank correlations were used as the test statistic. Second, clusters were defined as adjacent time samples that exhibited a statistically significant correlation ($r_s(n = 27) = .382, p = .05$, two-tailed), with cluster size corresponding to the sum of the correlation coefficients within a cluster. The variable "r_s^{mean}," defined as the average correlation for a given cluster, is reported to provide an assessment of the strength of the correlation for an entire cluster.

Figure 8A presents the correlations between individual differences in beta-band power versus differences in RT for the temporal anticipation effect, using power data from the left sensorimotor electrodes (see inset for electrodes). As can be seen, the correlation between power modulations and RT modulations tended to increase over the course of the delay period, being maximal around the time of anticipated go-cue occurrence at 2 sec. This was confirmed by a significant cluster spanning between 1912 and 2040 msec (size = 7.75, $p = .03$, $r_s^{\text{mean}} = .407$). This indicates that left sensorimotor beta-band power reflects a state of motor preparation whose relationship with RT peaks at the expected moment of go-cue. As a qualitative appreciation of the direction of the correlation, mean power modulations over the period of the significant cluster are plotted against RT modulations incurred by the temporal anticipation factor, for each individual participant (Figure 8B). As can be seen, participants for whom beta-band activity was most reduced by temporal anticipation tended to present the largest reductions in RTs, whereas those that presented the reverse pattern of beta-band modulations (i.e., increase in beta-band power under temporal anticipation) presented increases in RTs. The direction of the effect is thus consistent and complementary with the previously reported main effect of temporal anticipation observed at 1.25 sec. In summary, individual RT gains incurred through temporal anticipation were well accounted for by differences in beta-band modulations in the left sensorimotor regions, specifically around the moment of go-cue.

Figure 8C presents the correlations between individual differences in beta-band power versus differences in RTs for the spatial anticipation effect, using power data from

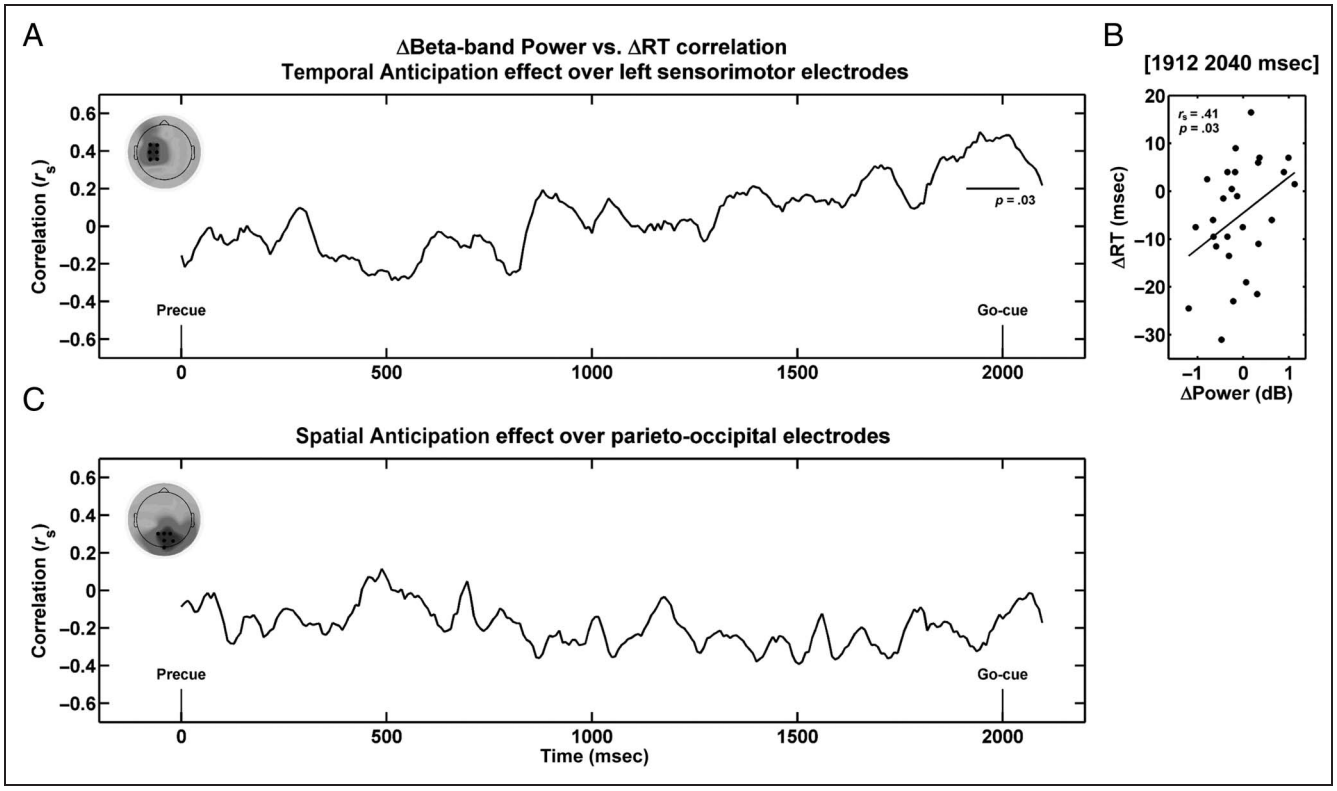

Figure 8. Correlations between beta-band power and RTs. (A) Time course of Spearman correlations between modulations in beta-band power incurred by temporal anticipation and associated modulations in RT across participants. Six electrodes overlaying left sensorimotor regions were used (same as in Figure 4B; see inset). Horizontal line corresponds to the time period during which the cluster was significant (1912–2040 msec; $p = .03$). (B) Mean power modulations over the period of the significant cluster plotted against RT modulations incurred by the Temporal Anticipation factor, for each individual participant ($n = 27$). (C) Time course of Spearman correlations between modulations in beta-band power incurred by spatial anticipation and associated modulations in RT across participants. Six electrodes overlaying parieto-occipital regions were used (same as in Figure 5B; see inset). No significant correlation was found.

the parieto-occipital electrodes (see inset for electrodes). As can be seen, no significant correlation was observed at any time during the delay period. This suggests that parieto-occipital beta-band power is not linked to the timing of movement initiation.

DISCUSSION

This study investigated whether the RT gains incurred by temporal and spatial anticipation are subtended by similar beta-band modulations during movement preparation. To do so, EEG activity was recorded in a reach RT task in which knowledge of the target spatial location and timing of onset was manipulated. Results revealed that although temporal and spatial anticipation both led to significant RT gains, they were subtended by modulations in beta-band activity in distinct regions and different time periods. In particular, only temporal anticipation incurred beta-band ERD over contralateral sensorimotor electrodes, the magnitude of which predicted RT modulations across participants. These findings argue for distinct states of motor preparation associated with temporal and spatial anticipation.

Temporal Anticipation Is Associated with Sensorimotor Beta-band Desynchronization

Temporal anticipation incurred greater beta-band ERD over contralateral sensorimotor regions specifically around the moment a go-cue was possible (i.e., ~1.25 sec in the *Three Timings* conditions). Interestingly, the magnitude of these beta-band modulations around the time of actual target onset (i.e., 2 sec) was correlated to the ensuing RT modulations across participants. These results are in line with the contention that beta-band oscillations signal the maintenance of the sensorimotor "status quo" (Engel & Fries, 2010) and conversely that a reduction in power indexes the degree to which a change is likely in the sensorimotor system (Kilavik et al., 2013; Jenkinson & Brown, 2011). In support, beta-band power over M1 has been shown to be progressively suppressed with the increasing likelihood of a go-cue instructing movement initiation (Schoffelen, Oostenveld, & Fries, 2005). It has been suggested that sensorimotor beta-band oscillations reflect interactions between the BG and M1 (Brittain, Sharott, & Brown, 2014), with desynchronization reflecting disinhibition and thus scaling with the time needed for movement initiation (Jenkinson & Brown, 2011; Kühn et al., 2004). As

such, Parkinson disease, for which a cardinal symptom is a difficulty in initiating movement, is characterized by abnormally high beta-band oscillations in both BG and M1 (Brown, 2007). Drug-induced reduction in beta-band activity in BG (Kühn, Kupsch, Schneider, & Brown, 2006) and sensorimotor cortex (Silberstein et al., 2005; Devos et al., 2003) is known to alleviate this symptom. Functionally, it has been proposed that premovement beta-band desynchronization allows to increase computational power and information coding within task-relevant neural ensembles (Brittain & Brown, 2014). As such, there is good evidence for an inverse relationship between firing rates within motor regions and beta-band power (van Wijk, Beek, & Daffertshofer, 2012; Spinks, Kraskov, Brochier, Umilta, & Lemon, 2008; Baker, Spinks, Jackson, & Lemon, 2001). Given that M1 cells undergo the most important change in firing specifically at movement initiation (Shenoy, Sahani, & Churchland, 2013; van Wijk et al., 2012), it is likely that the greater ERD observed over sensorimotor electrodes allowed for the timely allocation of neural resources at the critical moment associated with an imminent change in motor state.

The selective modulation of sensorimotor beta-band power with temporal anticipation of the upcoming target is particularly interesting in light of work from Kaufman et al. (2016), who found that the largest component of the neural response in M1 and dorsal premotor cortex reflects the timing of transition from movement preparation to initiation, independently of movement direction. Similar to the present results, they also reported that the timing of the change in neural state space predicted much of the trial-by-trial variance in RTs. Hence, a likely possibility is that sensorimotor beta-band activity is related to the temporally sensitive neurons identified by Kaufman and colleagues, with ERD allowing neuronal activity to converge into a state necessary for movement to be generated and thus correlating with RTs. In summary, the present findings support the view that beta-band ERD reflects processes that are needed to prompt responses to task-relevant stimuli (Perfetti et al., 2011) and marks the dissociation between movement preparation and initiation.

A null, yet potentially important, result of this work is that spatial anticipation did not impact premovement beta-band activity over contralateral sensorimotor regions, in spite of the fact that this factor led to more potent RT gains than temporal anticipation. Under the experimental conditions tested here, it suggests that sensorimotor beta-band desynchronization is more closely linked with movement initiation than with the encoding of the spatial aspects of movements. This view is consistent with evidence that EEG beta-band activity during the preparatory period yields poor directional decoding accuracy of hand movement direction (Waldert et al., 2008) and is not influenced by upcoming visual feedback direction (Dufour, Thénault, & Bernier, 2018). However, these results are inconsistent with those of Tzagarakis et al. (2010), who used magnetoencephalography (MEG) and found that beta-band desynchronization during planning negatively scaled with the directional uncertainty of an upcoming movement. One possible explanation lies in the different experimental designs. Indeed, in the present protocol, the target layout only spanned 120°, such that movements were systematically directed in the forward direction. This may have engaged neuronal ensembles broadly tuned to the forward direction to some extent in all conditions, even in the *Three Targets* condition (Cisek, 2006). In contrast, the target layout in Tzagarakis et al. (2010) spanned 360°, with targets being equally spaced around a circle. Such orthogonal target positioning likely prevented any possibility of encoding a movement vector in the high uncertainty context. As a result, the greater range of spatial uncertainty afforded by their design might have led to more potent beta-band modulations across conditions as compared with ours. Alternatively, it cannot be ruled out that the discrepant results stem from the different recording techniques, as EEG and MEG are sensitive to radial and tangential dipoles, respectively (Cohen, 2014; Hämäläinen, Hari, Ilmoniemi, Knuutila, & Lounasmaa, 1993). As such, it has been shown that the decoding of directional information during movement preparation differs between EEG and MEG (Waldert et al., 2008).

Spatial Anticipation Is Associated with Parieto-occipital Beta-band Synchronization

In further support for a dissociation between temporal and spatial anticipation, the latter incurred modulations at different scalp sites and with a different time course. Namely, spatial anticipation was associated with a sustained increase in beta-band power over parieto-occipital regions over the entire delay period, which was unrelated to ensuing RTs. This finding can be interpreted in light of the role of low beta-band oscillations (as well as alpha-band; 8–12 Hz) in regulating functional excitability within dorsal visual pathways for optimal task performance (Jensen & Mazaheri, 2010; Zhang, Wang, Bressler, Chen, & Ding, 2008; Donner et al., 2007). Specifically, when target location is precued, sensorimotor transformations can readily take place (Cappadocia, Monaco, Chen, Blohm, & Crawford, 2017), allowing to maintain a movement vector throughout the delay period (Bernier, Whittingstall, & Grafton, 2017; Andersen & Buneo, 2002; Buneo, Jarvis, Batista, & Andersen, 2002). In this context, the go-cue carries no novel visuospatial information and merely acts as a trigger, in which case it has been shown to be processed outside parietal regions (Bernier et al., 2017; Baldauf, Cui, & Andersen, 2008; Snyder, Dickinson, & Calton, 2006). In this light, increased beta-band power may reflect functional disengagement of visuospatial attention processes within parieto-occipital cortex given that sensorimotor transformations have already been computed.

Temporal Anticipation and RTs

Following the reasoning that temporal anticipation acts to reduce beta-band power, ERD should have been greater in *One Timing* as compared with *Three Timings* at ~2 sec, because there was a higher probability of a target being presented in the former condition. However, the analysis revealed no significant cluster at that moment (see Figure 4A). This is likely attributable to the relatively small difference in RTs incurred by temporal anticipation (5 msec, yet significant with an effect size deemed "large"), with a subset of participants even presenting the reverse effect (i.e., lower RTs in *Three Timings*; see *y*-axis of Figure 8B). It is well known that temporal anticipation can be described in terms of the hazard function, with a shortening of RTs at the longest delay periods due to the increasing probability for a target to appear as a function of time within a trial (Nobre et al., 2007; Luce, 1986). Despite the presence of no-go trials (which tend to counteract the effect of the hazard function), it is possible that the relatively small increase in RTs in the *Three Timings* conditions was partly attributable to this effect. Alternatively, in spite of evidence that constant delay periods tend to reduce RTs as compared with variable delay periods (Johari & Behroozmand, 2017; Alegria, 1975), one possibility is that the use of three fixed delay period durations with a constant interval was stereotyped enough to induce three distinct internal representations of go-cue occurrence. As a result, some participants might have entrained to multiple peaks of relatively high levels of preparation, consequently shortening their RTs. Yet, in spite of this behavioral reversal, it is noteworthy that these participants tended to present the reverse effect in sensorimotor beta-band activity (i.e., decreased beta-band power in *Three Timings*), as evidenced by the significant correlation between beta-band power and RT at ~2 sec. Hence, even though the manipulation of temporal anticipation had variable effects across participants, the entire data set supports the existence of a link between sensorimotor beta-band ERD incurred by temporal anticipation and associated RT modulations.

Conclusion

In conclusion, this study provides evidence for a dissociation between the effects of temporal and spatial anticipation on beta-band activity during movement planning. These data suggest that increasing "motor readiness" through spatial or temporal anticipation gives rise to fundamentally different brain states: one tonic process that is modulated by the spatial aspects of the movement and does not correlate with ensuing RTs and one phasic process that reflects the temporal likelihood to initiate the movement and therefore predicts RTs. More generally, these results support the notion of independence between movement preparation and initiation.

Acknowledgments

This work was supported by the Natural Sciences and Engineering Research Council (grant number 418589) and benefited from the CNRS for travel funds. The authors thank François Thénault for his significant technical contribution to this work.

Reprint requests should be sent to Pierre-Michel Bernier, Département de kinanthropologie, Faculté des sciences de l'activité physique, Université de Sherbrooke, 2500 Boulevard de l'Université, Sherbrooke, QC J1K 2R1, Canada, or via e-mail: pierre-michel.bernier@usherbrooke.ca.

REFERENCES

Alegre, M., Gurtubay, I. G., Labarga, A., Iriarte, J., Malanda, A., & Artieda, J. (2003). Alpha and beta oscillatory changes during stimulus-induced movement paradigms: Effect of stimulus predictability. *NeuroReport*, *14*, 381–385.

Alegria, J. (1975). Sequential effects of foreperiod duration as a function of the frequency of foreperiod repetitions. *Journal of Motor Behavior*, *7*, 243–250.

Andersen, R. A., & Buneo, C. A. (2002). Intentional maps in posterior parietal cortex. *Annual Review of Neuroscience*, *25*, 189–220.

Arnal, L. H. (2012). Predicting "when" using the motor system's beta-band oscillations. *Frontiers in Human Neuroscience*, *6*, 225.

Baker, S. N., Spinks, R. L., Jackson, A., & Lemon, R. N. (2001). Synchronization in monkey motor cortex during a precision grip task. I. Task-dependent modulation in single-unit synchrony. *Journal of Neurophysiology*, *85*, 869–885.

Baldauf, D., Cui, H., & Andersen, R. A. (2008). The posterior parietal cortex encodes in parallel both goals for double-reach sequences. *Journal of Neuroscience*, *28*, 10081–10089.

Bernier, P.-M., Whittingstall, K., & Grafton, S. T. (2017). Differential recruitment of parietal cortex during spatial and non-spatial reach planning. *Frontiers in Human Neuroscience*, *11*, 249.

Brainard, D. H. (1997). The Psychophysics Toolbox. *Spatial Vision*, *10*, 433–436.

Brittain, J.-S., & Brown, P. (2014). Oscillations and the basal ganglia: Motor control and beyond. *Neuroimage*, *85*, 637–647.

Brittain, J.-S., Sharott, A., & Brown, P. (2014). The highs and lows of beta activity in cortico-basal ganglia loops. *European Journal of Neuroscience*, *39*, 1951–1959.

Brown, P. (2007). Abnormal oscillatory synchronisation in the motor system leads to impaired movement. *Current Opinion in Neurobiology*, *17*, 656–664.

Buneo, C. A., Jarvis, M. R., Batista, A. P., & Andersen, R. A. (2002). Direct visuomotor transformations for reaching. *Nature*, *416*, 632–636.

Buzsáki, G. (2006). *Rhythms of the brain*. New York: Oxford University Press.

Cappadocia, D. C., Monaco, S., Chen, Y., Blohm, G., & Crawford, J. D. (2017). Temporal evolution of target representation, movement direction planning, and reach execution in occipital–parietal–frontal cortex: An fMRI study. *Cerebral Cortex*, *27*, 5242–5260.

Cisek, P. (2006). Integrated neural processes for defining potential actions and deciding between them: A computational model. *Journal of Neuroscience*, *26*, 9761–9770.

Cohen, J. (1988). *Statistical power analysis for the behavioral sciences* (2nd ed.). Hillsdale, NJ: Erlbaum.

Cohen, M. X. (2014). *Analyzing neural time series data: Theory and practice*. Cambridge, MA: MIT Press.

Delorme, A., & Makeig, S. (2004). EEGLAB: An open source toolbox for analysis of single-trial EEG dynamics including independent component analysis. *Journal of Neuroscience Methods*, *134*, 9–21.

Devos, D., Labyt, E., Derambure, P., Bourriez, J. L., Cassim, F., Guieu, J. D., et al. (2003). Effect of L-Dopa on the pattern of movement-related (de)synchronisation in advanced Parkinson's disease. *Clinical Neurophysiology*, *33*, 203–212.

Donner, T. H., Siegel, M., Oostenveld, R., Fries, P., Bauer, M., & Engel, A. K. (2007). Population activity in the human dorsal pathway predicts the accuracy of visual motion detection. *Journal of Neurophysiology*, *98*, 345–359.

Dufour, B., Thénault, F., & Bernier, P.-M. (2018). Theta-band EEG activity over sensorimotor regions is modulated by expected visual reafferent feedback during reach planning. *Neuroscience*, *385*, 47–58.

Engel, A. K., & Fries, P. (2010). Beta-band oscillations—Signalling the status quo? *Current Opinion in Neurobiology*, *20*, 156–165.

Field, A. P. (2009). *Discovering statistics using SPSS (and sex and drugs and rock 'n' roll)* (3rd ed.). London: Sage Publications.

Fritz, C. O., Morris, P. E., & Richler, J. J. (2012). Effect size estimates: Current use, calculations, and interpretation. *Journal of Experimental Psychology: General*, *141*, 2–18.

Fujioka, T., Trainor, L. J., Large, E. W., & Ross, B. (2012). Internalized timing of isochronous sounds is represented in neuromagnetic beta oscillations. *Journal of Neuroscience*, *32*, 1791–1802.

Gilbertson, T., Lalo, E., Doyle, L., Di Lazzaro, V., Cioni, B., & Brown, P. (2005). Existing motor state is favored at the expense of new movement during 13–35 Hz oscillatory synchrony in the human corticospinal system. *Journal of Neuroscience*, *25*, 7771–7779.

Grent-'t-Jong, T., Oostenveld, R., Jensen, O., Medendorp, W. P., & Praamstra, P. (2014). Competitive interactions in sensorimotor cortex: Oscillations express separation between alternative movement targets. *Journal of Neurophysiology*, *112*, 224–232.

Gwin, J. T., & Ferris, D. P. (2012a). An EEG-based study of discrete isometric and isotonic human lower limb muscle contractions. *Journal of Neuroengineering and Rehabilitation*, *9*, 35.

Gwin, J. T., & Ferris, D. P. (2012b). Beta- and gamma-range human lower limb corticomuscular coherence. *Frontiers in Human Neuroscience*, *6*, 258.

Gwin, J. T., Gramann, K., Makeig, S., & Ferris, D. P. (2010). Removal of movement artifact from high-density EEG recorded during walking and running. *Journal of Neurophysiology*, *103*, 3526–3534.

Haith, A. M., Pakpoor, J., & Krakauer, J. W. (2016). Independence of movement preparation and movement initiation. *Journal of Neuroscience*, *36*, 3007–3015.

Hämäläinen, M., Hari, R., Ilmoniemi, R. J., Knuutila, J. E. T., & Lounasmaa, O. V. (1993). Magnetoencephalography—Theory, instrumentation, and applications to noninvasive studies of the working human brain. *Reviews of Modern Physics*, *65*, 413–497.

Hammon, P. S., Makeig, S., Poizner, H., Todorov, E., & De Sa, V. R. (2008). Predicting reaching targets from human EEG. *IEEE Signal Processing Magazine*, *25*, 69–77.

Hick, W. E. (1952). On the rate of gain of information. *Quarterly Journal of Experimental Psychology*, *4*, 11–26.

Jenkinson, N., & Brown, P. (2011). New insights into the relationship between dopamine, beta oscillations and motor function. *Trends in Neurosciences*, *34*, 611–618.

Jensen, O., & Mazaheri, A. (2010). Shaping functional architecture by oscillatory alpha activity: Gating by inhibition. *Frontiers in Human Neuroscience*, *4*, 186.

Johari, K., & Behroozmand, R. (2017). Temporal predictive mechanisms modulate motor reaction time during initiation and inhibition of speech and hand movement. *Human Movement Science*, *54*, 41–50.

Jung, T.-P., Makeig, S., Humphries, C., Lee, T.-W., McKeown, M. J., Iragui, V., et al. (2000). Removing electroencephalographic artifacts by blind source separation. *Psychophysiology*, *37*, 163–178.

Kaufman, M. T., Seely, J. S., Sussillo, D., Ryu, S. I., Shenoy, K. V., & Churchland, M. M. (2016). The largest response component in the motor cortex reflects movement timing but not movement type. *eNeuro*, *3*, ENEURO.0085-16.2016.

Khanna, P., & Carmena, J. M. (2017). Beta band oscillations in motor cortex reflect neural population signals that delay movement onset. *eLife*, *6*, e24573.

Kilavik, B. E., Zaepffel, M., Brovelli, A., MacKay, W. A., & Riehle, A. (2013). The ups and downs of beta oscillations in sensorimotor cortex. *Experimental Neurology*, *245*, 15–26.

Kühn, A. A., Kupsch, A., Schneider, G.-H., & Brown, P. (2006). Reduction in subthalamic 8–35 Hz oscillatory activity correlates with clinical improvement in Parkinson's disease. *European Journal of Neuroscience*, *23*, 1956–1960.

Kühn, A. A., Williams, D., Kupsch, A., Limousin, P., Hariz, M., Schneider, G.-H., et al. (2004). Event-related beta desynchronization in human subthalamic nucleus correlates with motor performance. *Brain*, *127*, 735–746.

Lakens, D. (2013). Calculating and reporting effect sizes to facilitate cumulative science: A practical primer for *t* tests and ANOVAs. *Frontiers in Psychology*, *4*, 863.

Luce, R. D. (1986). *Response times: Their role in inferring elementary mental organization (No. 8)*. Oxford: Oxford University Press.

Makeig, S., Westerfield, M., Jung, T.-P., Enghoff, S., Townsend, J., Courchesne, E., et al. (2002). Dynamic brain sources of visual evoked responses. *Science*, *295*, 690–694.

Maris, E., & Oostenveld, R. (2007). Nonparametric statistical testing of EEG- and MEG-data. *Journal of Neuroscience Methods*, *164*, 177–190.

Niemi, P., & Näätänen, R. (1981). Foreperiod and simple reaction time. *Psychological Bulletin*, *89*, 133–162.

Nobre, A. C., Correa, A., & Coull, J. T. (2007). The hazards of time. *Current Opinion in Neurobiology*, *17*, 465–470.

Oostenveld, R., Fries, P., Maris, E., & Schoffelen, J.-M. (2011). FieldTrip: Open source software for advanced analysis of MEG, EEG, and invasive electrophysiological data. *Computational Intelligence and Neuroscience*, *2011*, 156869.

Pelli, D. G. (1997). The VideoToolbox software for visual psychophysics: Transforming numbers into movies. *Spatial Vision*, *10*, 437–442.

Perfetti, B., Moisello, C., Landsness, E. C., Kvint, S., Pruski, A., Onofrj, M., et al. (2011). Temporal evolution of oscillatory activity predicts performance in a choice-reaction time reaching task. *Journal of Neurophysiology*, *105*, 18–27.

Pfurtscheller, G., & Lopes da Silva, F. H. (1999). Event-related EEG/MEG synchronization and desynchronization: Basic principles. *Clinical Neurophysiology*, *110*, 1842–1857.

Rosenthal, R. (1984). *Meta-analytic procedures for social science research*. Beverly Hills, CA: Sage Publications.

Saleh, M., Reimer, J., Penn, R., Ojakangas, C. L., & Hatsopoulos, N. G. (2010). Fast and slow oscillations in human primary motor cortex predict oncoming behaviorally relevant cues. *Neuron*, *65*, 461–471.

Schmidt, R. A., & Lee, T. D. (2011). *Motor control and learning: A behavioral emphasis* (5th ed.). Champaign, IL: Human Kinetics.

Schoffelen, J.-M., Oostenveld, R., & Fries, P. (2005). Neural coherence as a mechanism of effective corticospinal interaction. *Science*, *308*, 111–113.

Shenoy, K. V., Sahani, M., & Churchland, M. M. (2013). Cortical control of arm movements: A dynamical systems perspective. *Annual Review of Neuroscience*, *36*, 337–359.

Silberstein, P., Pogosyan, A., Kühn, A. A., Hotton, G., Tisch, S., Kupsch, A., et al. (2005). Cortico-cortical coupling in Parkinson's disease and its modulation by therapy. *Brain*, *128*, 1277–1291.

Snyder, L. H., Dickinson, A. R., & Calton, J. L. (2006). Preparatory delay activity in the monkey parietal reach region predicts reach reaction times. *Journal of Neuroscience*, *26*, 10091–10099.

Spinks, R. L., Kraskov, A., Brochier, T., Umilta, M. A., & Lemon, R. N. (2008). Selectivity for grasp in local field potential and single neuron activity recorded simultaneously from M1 and F5 in the awake macaque monkey. *Journal of Neuroscience*, *28*, 10961–10971.

Tzagarakis, C., Ince, N. F., Leuthold, A. C., & Pellizzer, G. (2010). Beta-band activity during motor planning reflects response uncertainty. *Journal of Neuroscience*, *30*, 11270–11277.

van Wijk, B. C. M., Beek, P. J., & Daffertshofer, A. (2012). Neural synchrony within the motor system: What have we learned so far? *Frontiers in Human Neuroscience*, *6*, 252.

Waldert, S., Preissl, H., Demandt, E., Braun, C., Birbaumer, N., Aertsen, A., et al. (2008). Hand movement direction decoded from MEG and EEG. *Journal of Neuroscience*, *28*, 1000–1008.

Zhang, Y., Wang, X., Bressler, S. L., Chen, Y., & Ding, M. (2008). Prestimulus cortical activity is correlated with speed of visuomotor processing. *Journal of Cognitive Neuroscience*, *20*, 1915–1925.